

Determination of the Absolute Orientation of Langatate Crystals Using X-ray Diffraction

B.T. Sturtevant¹, M. Pereira da Cunha², R.J. Lad¹
 Dept. of Physics¹ and Dept. of Electrical & Computer Engineering²
 Laboratory for Surface Science & Technology
 University of Maine, Orono, Maine USA
 rjlad@maine.edu

Abstract— Acoustic wave propagation in piezoelectric crystals with point group 32 symmetry is strongly dependent on the specific crystal orientation. This paper reports an X-ray diffraction (XRD) method using pole figures and in-plane scattering measurements to precisely define the absolute orientation of crystal planes in langatate (LGT). XRD measurements were conducted on Z-cut and $\pm 45^\circ$ Y-rotated LGT wafers whose absolute orientation had previously been determined by ultrasonic measurements. A large inequality in XRD intensity from certain LGT planes allows $\{hk \cdot l\}$ crystal orientations to be distinguished from $\{hk \cdot \bar{l}\}$ orientations. Specific Miller planes useful for LGT crystal alignment and absolute orientation by XRD are reported, along with the measured intensity ratios $I_{\{hk \cdot l\}} / I_{\{hk \cdot \bar{l}\}}$.

Keywords- langatate; absolute orientation; X-ray diffraction

I. INTRODUCTION

In crystals exhibiting point group 32 symmetry, such as quartz, gallium phosphate, and the LGX family (langasite, langanite, langatate), bulk acoustic waves (BAWs) traveling in the Y-Z plane and making an angle of α with the Z axis do not in general have the same phase velocity as BAWs traveling at an angle of $-\alpha$. Similarly, surface acoustic wave (SAW) propagation is sensitive to which side of the wafer is polished, particularly when the orientation exhibits non-zero power flow angle. Therefore, the absolute crystallographic orientation of this class of acoustic wave materials must be precisely known in order to characterize specific crystal wafer cuts, optimize device design, and correctly fabricate devices. This paper reports a simple, non destructive means for determining the positive axes of langatate (LGT, $\text{La}_3\text{Ga}_5.5\text{Ta}_{0.5}\text{O}_{14}$) crystals, and the method has enabled our recent work on accurate measurements of a full set of LGT acoustic wave constants and temperature coefficients [1].

The polarity of the crystalline X axis of an LGT crystal can be found by measuring the electric potential across the X faces induced by mechanical compression along the same axis, as prescribed in [2]. Mechanically squeezing a crystal, however, is only practical in the very early stages of sample preparation and an alternative method is highly desirable at later stages. X-ray diffraction (XRD) is a characterization tool that is unique compared to mechanical and optical methods in that it is completely non-destructive, it can be performed on samples of

a wide range of physical dimensions and orientations, and it can be performed on a sample which has roughened, polished, or even metalized faces. For these reasons, measurements of the precise orientation can be conducted at any stage of sample or device preparation.

Due to the mismatch between the symmetry of the lattice and the symmetry of the crystal, it is reported for some lattice planes in a class 32 crystal, such as quartz, that $I_{\{hk \cdot l\}} \neq I_{\{hk \cdot \bar{l}\}}$ where 'I' is the intensity of a diffracted X-ray beam off planes with Miller indices $\{hk \cdot l\}$ or $\{hk \cdot \bar{l}\}$ [3]. We adopt here the convention of abbreviating the fourth hexagonal Miller-Bravais index, $i = -h - k$, with a dot. In addition, if the X-ray wavelength is near an absorption edge, anomalous scattering effects cause $I_{\{hk \cdot l\}} \neq I_{\{\bar{h}\bar{k} \cdot \bar{l}\}}$. In other words, the measured diffraction intensity from a single set of planes depends on whether one is diffracting off the "top" or "bottom" of the planes [4].

The alignment and characterization of quartz crystals using X-rays has been the focus of significant effort [3-7] and has been highly motivated by industrial applications demanding process and quality control. As a result of this work, efficient data collection protocols have been established for determining the orientation of a piezoelectric crystal in any symmetry group [3-6]. Additionally, tables exist for $\{hk \cdot l\} / \{hk \cdot \bar{l}\}$ XRD intensity ratios for quartz [7]. While protocols exist for determining the absolute orientation of class 32 crystals, the specific X-ray reflections exhibiting intensity inequalities for quartz do not translate directly from quartz to other crystals such as LGT. Further, anomalous scattering effects are much more pronounced for LGT than for quartz because it is composed of heavier elements and thus has absorption edges closer to the wavelength of the Cu K α radiation used in this work.

II. EXPERIMENTAL PROCEDURE

A. Samples

An optically polished Z-cut quartz wafer was used to verify intensity differences between different crystal planes as reported in the literature [7]. Five different LGT samples were used in this work. Three wafers were optically polished and oriented with surface normals Y+45°, Y-45°, and Z. Two unpolished Z-cut and X-cut wafers were measured and these

This work was supported by AFOSR grant # FA9550-07-1-0519. BS also acknowledges support from NSF IGERT Grant # 0504494. The XRD instrumentation was funded by NSF MRI grant # 0521043.

wafers had an RMS roughness on the order of $1\mu\text{m}$. Alignment of each sample cut was controlled and verified by the method described in [8]. The alignment precision of each of the samples was better than 0.1° .

B. X-ray Pole Figures

A PANalytical X'Pert Pro MRD X-ray diffractometer operating in point focus configuration with $\text{Cu K}\alpha$ radiation was used in all measurements. The standard Φ , Ψ , θ , and ω are used to label the four degrees of freedom of the instrument [9]. High-Resolution Pole Figure (HRPF) measurements were acquired by fitting the instrument with a $(10\times 10)\text{mm}^2$ aperture poly-capillary X-ray lens on the incident beam side and a 0.18° parallel plate collimator with 0.02 rad Soller slits on the diffracted beam side.

For each pair of $\{hk \cdot l\}$, $\{hk \cdot \bar{l}\}$ planes investigated, a pole figure spanning 90° in Ψ and 360° in Φ was collected. An example of one of these scans from LGT $\{50 \cdot 2\}$ planes is shown in Fig. 1. The 2θ value used for pole figures was taken from ICDD PDF database card #00-047-0532 for each particular set of planes [10]. While these scans are useful for confirming the general orientation of the planes, the coarse resolution of 4° steps in Φ and 3° in Ψ is not useful for accurate intensity measurements. For quantitative comparison of diffracted intensities from each pole, HRPFs were collected around each of the six poles in Fig. 1. The HRPF measurements scanned 4° in Ψ ($0.1^\circ / \text{step}$) and 2° in Φ ($0.05^\circ / \text{step}$). During HRPF data acquisition, the diffractometer remained fixed in Ψ and the scan axis was Φ . Ψ was then incremented by 0.1° and another Φ scan was collected.

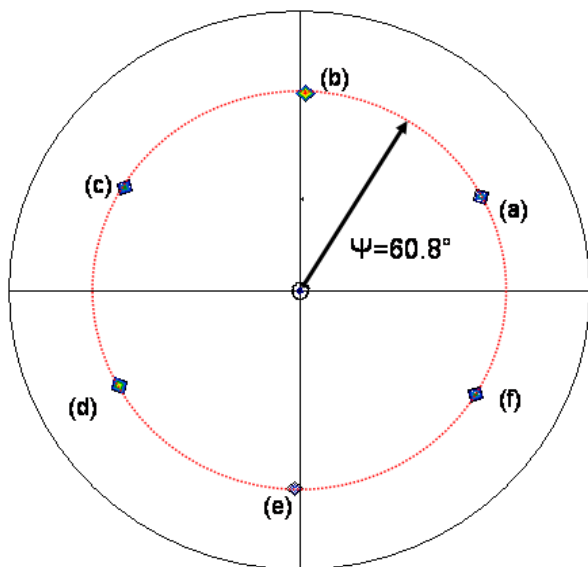


Figure 1. $\{502\}$ pole figure measured at $2\theta = 76.341^\circ$ from a Z-cut LGT wafer. Radial coordinate: $0 \leq \Psi \leq 90$; azimuthal coordinate: $0 \leq \Phi \leq 360$. Six equally spaced poles are present at 60.8° .

C. In-Plane Diffraction

In-Plane Diffraction (IPD) is very useful for probing crystal planes which are oriented perpendicular to the surface of a wafer [11]. In this work, XRD intensities from the X planes of a Z-cut wafer were measured. The optics for the IPD measurements were the same as for the HRPF measurements except that the aperture of the X-ray lens was reduced to $(3\times 2)\text{mm}^2$. An angular offset was introduced to the instrument such that $\omega = 90^\circ$ for the in-plane geometry. The 2θ was chosen appropriately for the plane under investigation, such as the $\{11 \cdot 0\}$. Ψ was inclined by $< 1.5^\circ$ from 90° so that the X-rays were incident at a very grazing angle to the surface. The scanned axis in an IPD measurement is the azimuthal coordinate, Φ , and can be varied from 0 to 360° . It should be noted that because IPD probes only the very near surface of a sample, specimens whose surfaces are polished to an optical finish yield much higher diffracted intensities than those with rougher surfaces.

III. RESULTS AND DISCUSSION

A. Pole Figures from Z-cut LGT Wafer

The data from an HRPF can be visualized on a 1D plot in which the horizontal axis is the Φ position and each trace corresponds to a different Ψ position (Fig. 2a). Alternatively, one can visualize the HRPF as a surface plot in which the two axes in the plane are Ψ and Φ while the height above the plane is the measured intensity (Fig. 2b). An advantage of the surface plot is that it is immediately obvious to the data collector whether or not the maximum diffracted intensity is included within the limits of both Ψ and Φ . For each HRPF, the peak parameters of the Φ scan with the highest measured intensity were determined and the net height of this peak was recorded. Maximum intensity Φ scans ($\Psi = 60.8^\circ$) from each of the six $\{50 \cdot 2\}$ HRPFs measured from Z-cut LGT are plotted together in Fig. 3. The letters (a)-(f) in the figure correspond to the six poles shown in Fig. 1.

Six HRPFs were measured from each of 13 different $\{hk \cdot l\}$ and $\{hk \cdot \bar{l}\}$ LGT planes. Since there is a three-fold rotational symmetry about the Z axis of the crystal (Fig. 3) with different intensities corresponding to either the $\{hk \cdot l\}$ or $\{hk \cdot \bar{l}\}$ planes, an average was taken of the intensities of the three equivalent planes and the ratio of these averages was recorded. Table 1 shows these intensity ratios along with the inclination from the Z axis for the 13 pairs of LGT poles that were measured. The table also shows our measured intensity ratios from quartz $\{04 \cdot 4\}$ and $\{05 \cdot 2\}$ planes which are consistent with the reported literature values [7].

B. Pole Figures from Singly Rotated LGT Wafers

Pole figures from $\{50 \cdot 2\}$ planes were measured on both $Y+45^\circ$ and $Y-45^\circ$ LGT wafers whose orientations had already been established by ultrasonic methods. Fig. 4 shows a low-resolution pole figure which is representative of both rotated cuts. In the figure, the letters Z and Y have been added to indicate the general orientation of the crystal (note that the same letter Y indicates the +Y direction in the case of a $Y+45^\circ$

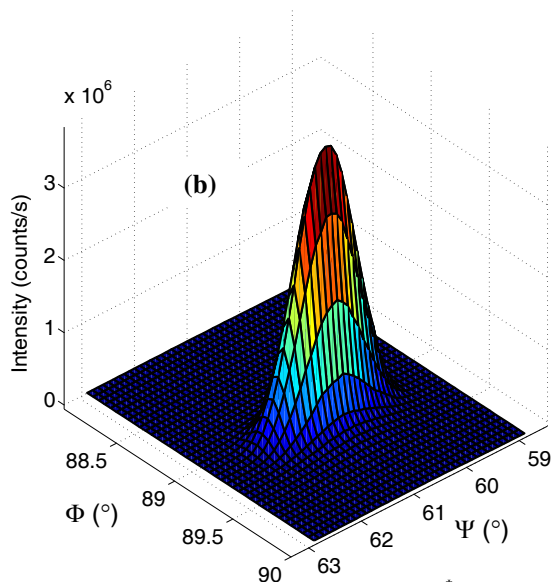
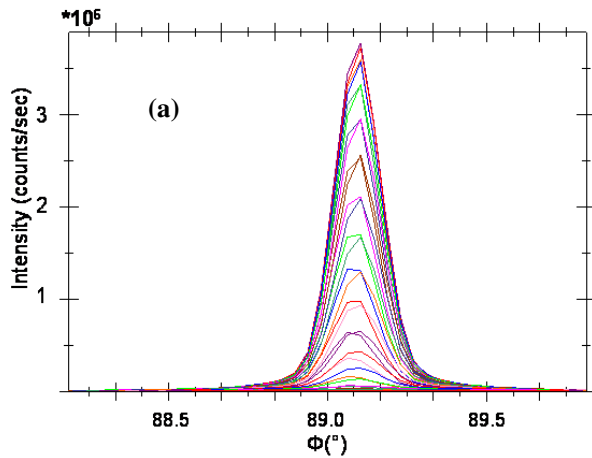


Figure 2. (a) A high-resolution pole figure displayed in 1-D. Each trace is a scan in Φ while Ψ remains fixed. Ψ is varied by 0.1° from one trace to another. (b) A high-resolution pole figure displayed as a surface plot.

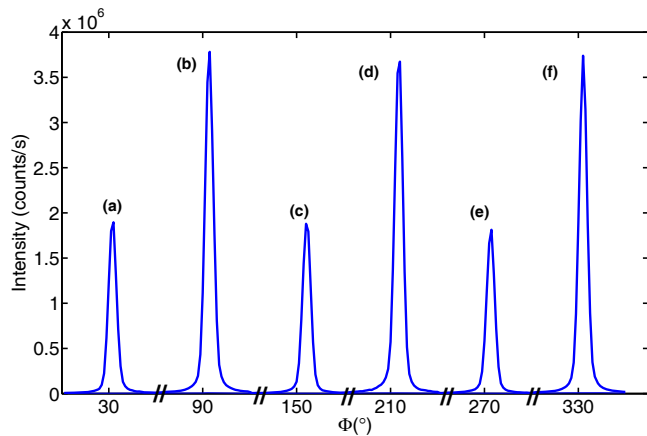


Figure 3. Maximum intensity Φ scans ($\Psi=60.8^\circ$) for each of the six LGT $\{50\cdot 2\}$ poles labeled (a)-(f) in Fig. 1. The FWHM for each peak is $\sim 12^\circ$.

TABLE I. INCLINATION FROM THE Z-AXIS AND XRD INTENSITY RATIOS FOR LGT CRYSTAL PLANES

$\{hk\cdot l\}$	α ($^\circ$) ^a	$I_{(+)} / I_{(-)}$
$\{10\cdot 1\}$ ^b	35.72	2.08
$\{10\cdot 2\}$	19.77	0.95
$\{20\cdot 1\}$	55.19	0.92
$\{20\cdot 2\}$	35.72	1.57
$\{20\cdot 3\}$	25.61	0.77
$\{20\cdot 4\}$	19.77	3.09
$\{30\cdot 1\}$	65.13	0.23
$\{30\cdot 2\}$	47.17	1.00
$\{30\cdot 4\}$	28.34	0.95
$\{40\cdot 2\}$	55.19	0.39
$\{40\cdot 3\}$	43.79	8.23
$\{50\cdot 1\}$	74.46	0.77
$\{50\cdot 2\}$	60.91	1.86
QTZ ^c $\{04\cdot 4\}$	51.78	15.8 (17.1 ^d)
QTZ $\{05\cdot 2\}$	72.52	0.03 (0.01 ^d)

a) α denotes the angle of the plane's normal with respect to the Z axis.

b) boldfaced indicates planes whose diffracted intensities differ by at least a factor of two.

c) QTZ denotes planes measured on quartz samples. All other planes measured on LGT.

d) reported in [7].

cut and it represents -Y in the case of a Y-45° cut). HRPFs (not shown) were collected in the regions (i), (ii), and (iii) indicated in the figure. As expected, the maximum measured intensity in regions (i) and (iii) were similar to each other and were markedly different from the maximum measured intensity in region (ii). The average intensity of regions (i) and (iii) was compared to the measured intensity from region (ii) and it was found in the case of the Y+45° cut that $I_{i,iii}/I_{ii}=1.28$ while the same ratio measured 0.46 in the case of the Y-45° cut.

Although the specific cut can be clearly identified by the observed intensity ratios, it should be noted that the $I_{i,iii}/I_{ii}$ ratio for the Y-45° cut is not the reciprocal of the same ratio for the Y+45° cut. As discussed in [7], the diffracted intensity measured from a plane diminishes as the angle between the crystallographic plane and the actual surface increases due to absorption effects. Thus, when the planes in regions (i) and (iii) naturally diffract more strongly than the plane in region (ii), the intensity ratio is brought closer to unity than it would be if all the planes were inclined with respect to the surface by the same amount (as is the case for a Z-cut wafer). If the plane in region (ii) diffracts more strongly, the ratio is brought further from unity than it would be if all the planes were inclined with respect to the surface by the same amount. This geometrical attenuation factor makes it important, when determining orientation, to use planes which have diffracting powers that are as different as possible from each other such as those planes listed by boldface in Table 1. From the position of the poles in a low-resolution pole figure, one can easily determine the inclination of the sample surface normal with respect to the

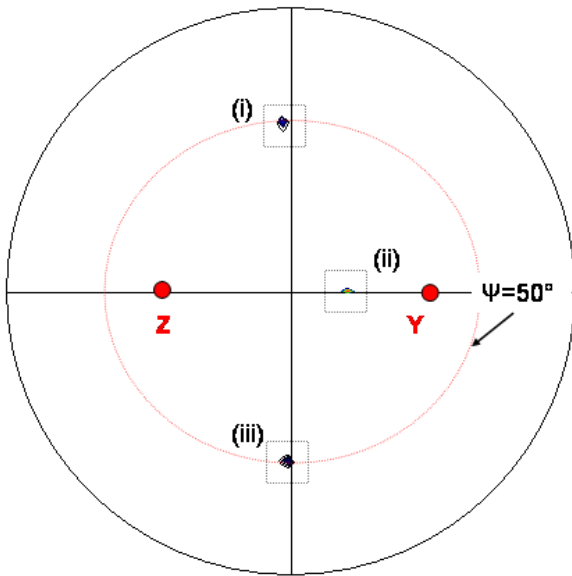


Figure 4. A low resolution $\{50 \cdot 2\}$ pole figure typical of either a $Y+45^\circ$ or $Y-45^\circ$ rotated LGT sample. The letters Z & Y indicate the general orientation of these poles (note for a $+45^\circ$ cut, 'Y' indicates the +Y direction, while the opposite holds for a -45° cut). HRPFs were collected in the three regions indicated.

different axes. However, by using a HRPF and comparing the intensities measured from different poles, one can determine the *sign* of the inclination with respect to the Z axis.

C. In-Plane Diffraction

Using the IPD technique, the scattering intensities from $\{11 \cdot 0\}$ LGT planes were measured on both an optically polished and an unpolished sample. Fig. 5 displays the data from the optically polished sample. As shown in the figure, the measured intensity from the +X $\{\bar{1}\bar{1} \cdot 0\}$ face was found to be about five times stronger than that from the '-X' $\{11 \cdot 0\}$ face. The ratio measured on the unpolished sample was the same, but the absolute intensities were higher from the polished sample by more than an order of magnitude owing to the high surface sensitivity of the measurement.

To confirm the result that the diffracted intensity from the +X face is stronger than that from the -X face, the HRPF intensity from each face of an unpolished X cut wafer was measured. In this HRPF measurement, scans were taken over all Φ angles and Ψ was varied from $89-90^\circ$ to ensure that a slight sample misalignment did not affect the results. The maximum intensities obtained from each side of the wafer were compared and found to be in the same ratio as in the IPD measurements.

IV. CONCLUSIONS

X-ray diffraction intensity measurements from several $\{hk \cdot l\}$ Miller planes have been accurately measured and used to yield the absolute crystal orientation of several LGT crystal wafers. 13 LGT poles were measured using high-resolution pole figures and the relative intensities from $\{hk \cdot l\}$ and $\{hk \cdot \bar{l}\}$ exhibit a wide range of relative intensities, which

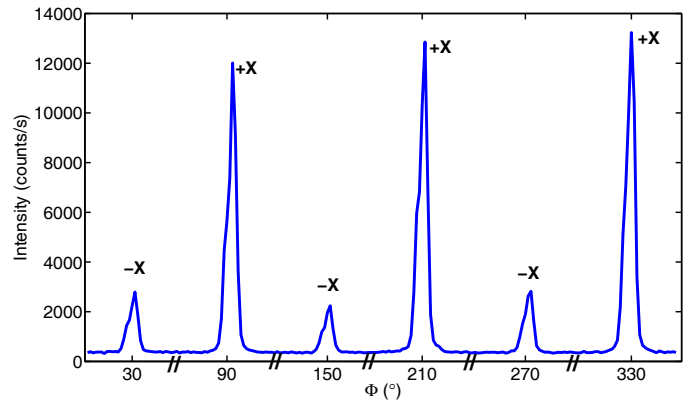


Figure 5. In plane diffraction Φ scan measured on Z-cut LGT showing clear intensity differences between diffraction from +X and -X faces. The FWHM of each curve is $\sim 3^\circ$.

enables the specific crystallographic axes to be determined. In-plane diffraction was used to measure the diffracted intensity from the six $\{11 \cdot 0\}$ poles. The intensity of diffracted X-rays from the $\{\bar{1}\bar{1} \cdot 0\}$ face was found to be about five times larger than that from the $\{11 \cdot 0\}$ face. This ratio was confirmed by diffraction off of both sides of an X-cut wafer.

ACKNOWLEDGMENT

The authors thank David Frankel of LASST for valuable discussions.

REFERENCES

- [1] B.T. Sturtevant, P.M. Davulis, M. Pereira da Cunha, "Pulse Echo and Combined Resonance Techniques: a Full Set of LGT Acoustic Wave Constants and Temperature Coefficients," IEEE Trans. Ultrason., Ferroelect., Freq. Cont., in press.
- [2] "Standards on Piezoelectric Crystals, 1949," Proc. IRE 37, 1949, pp 1378-1395.
- [3] J. F. Darces, J. Lamboley, and H. Merigoux, "Dissymmetry used for Φ , Θ angle sign determination of a piezoelectric crystal blank by a non-destructive method," Ferroelectrics, vol 40, pp 245-248, 1982
- [4] H. Merigoux, J. F. Darces, and J. Lamboley, "X-ray handedness determination on finished doubly rotated quartz plates," Proc. 1984 IEEE Int'l. Freq. Cont. Symp., pp 496-498.
- [5] H. Berger, H.-A. Bradaczek, and G. Hildebrandt, "Further Progress in the absolute orientation determination of double rotated quartz blanks by the means of the Ω -scan method," Proc. 2001 IEEE Int'l. Freq. Cont. Symp., pp 393-395.
- [6] J. F. Darces and H. Merigoux, "Final X-ray control of the orientation of round or rectangular quartz slides for industrial purposes," Proc. 1978 IEEE Int'l. Freq. Cont. Symp., pp 304-309.
- [7] W.L. Bond and E.J. Armstrong, "The Use of X-rays for Determining the Orientation of Quartz Crystals," in *Quartz Crystals for Electrical Circuits, Their Design and Manufacture*, Raymond A. Heising, Ed. D. Van Norstrand Company, Inc., 1952, pp 95-139.
- [8] L. D. Doucette, M. Pereira da Cunha, R. J. Lad, "Precise orientation of single crystals by a simple x-ray diffraction rocking curve method," Rev. Sci. Instr., vol. 76, 036106, (4 pages), 2005.
- [9] M. Birkholz, *Thin Film Analysis by X-ray Scattering*, 2nd ed., Wiley-VCH: Weinheim, 2006.
- [10] PDF-4+ 2007 Database, International Centre for Diffraction Data, Newton Square, PA, <http://www.icdd.com>.
- [11] P. Fewster, *X-ray Scattering from Semiconductors*, 2nd ed., Imperial College Press, 2003.